FINAL SCIENTIFIC/TECHNICAL REPORT

COVER PAGE INFORMATION

Report Submitted to:	U.S. Department of Energy
Contract #:	DE-SC0011255
Project Title:	Low Loss Graded Index Polymer Optical Fiber for Local Networking
Principal Investigator:	Richard Claus 540-626-6266 office phone roclaus@nanosonic.com
Submission Date:	5 April 2018
DUNS Number:	008963758
Recipient Organization:	NanoSonic Inc. 158 Wheatland Drive Pembroke, VA 24136
Project Period:	06 April 2015 to 05 February 2018
Reporting Period End Date:	05 April 2018
Report Frequency:	Semi-annual

Signature:

TABLE OF CONTENTS

I. EXECUTIVE SUMMARY

The objective of this Department of Energy SBIR program has been to develop technology for the advancement of advanced computing systems. NanoSonic worked with two subcontractors, the Polymicro Division of Molex, a U.S.-based manufacturer of specialized optical fiber and fiber components, and Virginia Tech, a research university involved through the Global Environment for Network Innovations (GENI) program in high-speed computer networking research. NanoSonic developed a patented molecular-level self-assembly process to manufacture polymer-based optical fibers in a way similar to the modified chemical vapor deposition (MCVD) approach typically used to make glass optical fibers. Although polymer fiber has a higher attenuation per unit length than glass fiber, short connectorized polymer fiber jumpers offer significant cost savings over their glass counterparts, particularly due to the potential use of low-cost plastic fiber connectors. As part of the SBIR commercialization process, NanoSonic exclusively licensed this technology to United Technologies, a large ($100B+ market cap) U.S.-based manufacturing conglomerate near the end of the first year of the Phase II program. With this base technology developed and licensed, NanoSonic then worked with Molex/Polymicro to address secondary program goals of using related but not conflicting production methods to enhance the performance of other specialty optical fiber products and components, and Virginia Tech continued its evaluation of developed polymer fibers in its network infrastructure system on the university campus. We also report our current understanding of the observation during the Phase I program of quantum conductance and partial quantum conductance in metal-insulator-metal (MIM) devices. Such conductance behavior may be modeled as singlemode behavior in one-dimensional electrically conducting waveguides, similar in principle to singlemode optical propagation in dielectric fiber waveguides. Although NanoSonic has not licensed any of the additional technology developed during the second year of the program, several proprietary discussions with major materials companies are underway as of the conclusion of Phase II.

II. SBIR PROGRAM ACCOMPLISHMENTS

The major accomplishments of this Phase II SBIR program have been

- the licensing of one of our polymer optical fiber materials and the process used to manufacture it to the United Technologies Corporation (UTC, www.utc.com) for a broad field of use, and
- a first right of refusal agreement with Schlumberger (www.slb.com) for a slightly different polymer and a separate field of use.

UTC was made aware of our material through our connection with Sikorsky Aircraft, now a part of Lockheed Martin, as noted in our DOE Phase II SBIR proposal. UTC optical scientists visited NanoSonic, and NanoSonic engineers visited UTC's microelectronics and optoelectronics manufacturing facility in Minneapolis prior to creating the license agreement. Schlumberger was made aware of our material through the DOE SBIR website and they contacted NanoSonic directly. It should be noted that commercialization specialists at Dawnbreaker Inc. provided much advice and suggestions during the development of licensing agreements with both UTC and Schlumberger.

Additionally, recent work that does not conflict with either the UTC or Schlumberger agreements has led to the development of three new prototype fiber materials that have been evaluated by the Polymicro Division of our Phase II subcontractor, Molex Inc. Polymicro manufactures specialized optical fibers for a number of niche markets. During the final few months of the Phase II program, NanoSonic revisited the observation of electron propagation in one-dimensional metal waveguides and that has been of interest to engineers at Honeywell Inc. for potential use in low power electronic devices.

Further, we have an NDA in place and have held initial proprietary licensing discussions with AkzoNobel ($20B market cap, https://www.akzonobel.com), the world's largest coatings and specialty chemicals company, and have preliminary proprietary discussions underway with Johns Manville, a Berkshire Hathaway company ($20B market cap, http://www.jm.com) and Sherman Williams, a well known paint and coatings company ($31B market cap, https://www.sherwin-williams.com).

a. What are the major goals of the project?

The primary initial objective of this DOE SBIR program was to develop ultra-low loss, and low cost, graded index polymer optical fibers (GI-POF) and components for high-speed local area interconnects.

The three primary initial supporting technical and commercialization goals of the program were to produce

1. GI-POF that outperforms currently available products in terms of bandwidth-distance product and zero-dispersion wavelength range, while retaining low bend loss, ease of handling and splicing advantages, and the future potential to move to polymer singlemode at costs less than approximately $1/m,
2. Fiber that is non-flammable, non-flame spread, and low smoke, zero halogen (LSZH) for building local area network (LAN) interconnects, and
3. Low-cost connectorized polymer fiber jumper cables.

During the Phase II program, NanoSonic met these initial program goals and licensed the developed optical fiber materials technology to United Technologies. Without conflicting with that licensing agreement, we continued to work to develop additional optical fiber materials and manufacturing processes, specifically with input from our Phase II subcontractor Molex/Polymicro, and with input from other large materials companies. The applications of these materials and processes are in specialized optical fibers and in broader areas requiring coatings with specific engineering constitutive properties.

In particular, our Molex/Polymicro Phase II subcontractor recommended pursuing the development of specialized optical fibers having multiple commercial product requirements, as follows.

1. Low H_2 Permeability Coatings – Ideally this coating would have hydrogen permeability approximately the same as the ~300 angstrom carbon coating currently applied to optical fiber with a temperature rating of ≥150°C. The coating could of course be of greater thickness than the carbon, with a good target thickness being in the range of 75µm to 1000µm. Low hydrogen permeability coatings would be useful in extending the useable lifetime of hydrogen-loaded fibers used to manufacture in-line wavelength-selective fiber Bragg gratings (FBGs) used in WDM communication networks and optical fiber sensor systems.

It should be noted that Polymicro's interest in low hydrogen permeability materials led NanoSonic to separately consider the use of such low hydrogen permeable materials in very different applications of interest to the Department of Energy. Specifically, NanoSonic has developed flexible, high-pressure hoses for the delivery of hydrogen to fuel cell cars. Commercially we have only one competitor worldwide – SpirStar in Germany – but their hoses fail at a high rate so are not widely accepted.

2. Higher Temperature Polyimide Coating – The current polyimide fiber coatings are generally good for use at 300 to 350°C continuously with excursions to 400°C depending on exact conditions. A possible target would be to improve this thermal stability by 30 to 50°C. One possible path may be to have an outer polyimide layer that is "loaded" to

provide additional thermal stability.

It should be noted here that Polymicro's interest in high temperature fiber coating materials has also indirectly contributed to NanoSonic's consideration of similar high temperature coatings for other applications. We are currently manufacturing a proprietary large order of such material for a division of a large U.S.-based $96B market cap located in Florida.

3. Metal-Like Coating – NanoSonic has technology involving "Metal Rubber," an electrically conductive, low modulus material. If this technology could be converted into a liquid coating format that could be applied and cured on the fiber draw line, it could result in an interesting optical fiber with a very robust coating which is conductive/shielding, possibly higher temperature, high thermal barrier, and very abrasion resistant in a relatively small form factor.

4. UV Transparent Coating – A coating which has good optical transparency (>20%) down to the 300-355nm range when the coating thickness is on the order of 15 – 50µm. Specifically, Molex would like the transmission to be better than 10% at approximately 70-micron thickness at 300nm. Such a coating would allow more efficient writing of in-line fiber Bragg gratings (FBGs).

5. Multilayers on Inside of Capillary Tube – There are two types here of interest:

a. A Teflon-like, non-wetting coating, ideally 100 angstroms to 0.5µm thick on the ID of a flexible capillary. The capillary ideally would have an ID of 50 – 300µm. The coating would have to be non-wetting and offer reasonable stability with an aqueous/organic buffer solution that is in the pH range of 2 – 11.

b. A coating with a refractive index lower than water which is 1 to 2µm thick when deposited on the ID of a capillary. The refractive index of the coating material must be lower than the refractive index of water such that waveguide transmission will be supported through the water in the ID of the capillary. The target ID of the capillary is 250-670µm. The coating should have good UV transmission and be non-solarizing.

During the Phase II program, we considered these opportunities with Polymicro, and progress with several of these fiber materials is summarized later in this report.

Our Schlumberger partner is interested in polymer fibers and polymer fiber materials because of their potential mechanical flexibility in comparison to conventional glass fibers for use in downhole oil and gas exploration and data transmission.

AkzoNobel, Sherman Williams and Johns Manville are interested in coating materials with slightly different properties, although our current NDAs with them do not allow us to indicate their specific commercial goals. Part of our commercialization objective is to

conclude non-conflicting licensing agreements with all of them to maximize the long-term profit resulting from this DOE program.

b. What was accomplished under these goals?

This section is divided into four major discussions that address work performed sequentially during the course of the Phase II program. Deviating slightly from the numbering format of the Final Report, these discussions are numbered II.A., II.B., II.C., and II.D. so they fit into the Table of Contents.

II.A. Addressing the Initial Development Goals of the Phase II Program

The initial goal of the Phase II program was to develop low loss polymer fiber using the layer-by-layer deposition technique demonstrated during Phase I. To begin this work, we synthesized a library of UV-curable polymers having different refractive indices; these are the materials that constitute the core and cladding of the polymer optical fiber. The use of photo- or UV- polymerization is a significant advantage as it offers the advantages of

i. fast drying times,
ii. opportunity for broad formulation range,
iii. low energy consumption, and
iv. low space and capital requirements for curing equipment [1-3].

Furthermore, UV-curable coatings are a class of polymer with little to no volatile organic compounds [4].

The main components of UV-curable coatings are an oligomer, a monomer, and a photoinitiator. We initially designed and synthesized fluorinated oligomers having a polyurethane acrylate structure. Figure 1 shows the synthetic route for making the polyurethane acrylate oligomers.

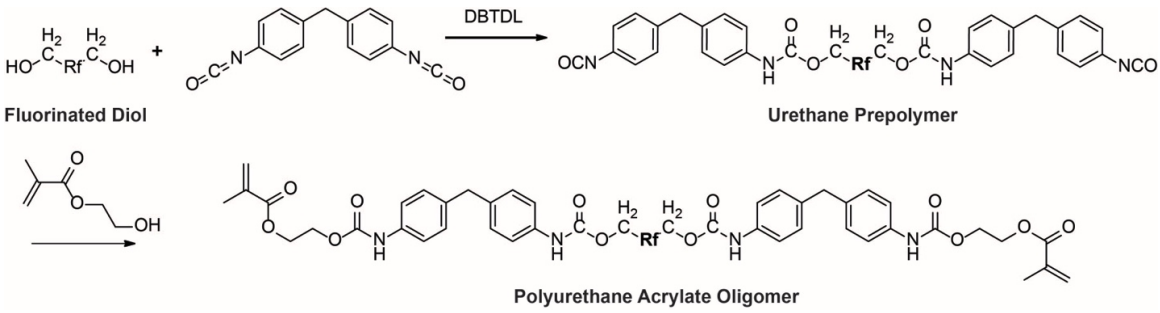

Figure 1: Synthesis of fluorinated polyurethane acrylate oligomer used in the core and cladding of polymer optical fiber.

The fluorinated oligomers were synthesized successfully in two steps. First, we reacted a carbodiimide-modified 4, 4-'diphenylmethane diisocyanate with a diol in toluene at 60°C using dibutyltin dilaurate (DBTDL) as a catalyst. The urethane prepolymer was then reacted with 2-hydroxyethyl methacrylate (HEMA), and completion of the reaction was monitored by IR spectroscopy for disappearance of the isocyanate group (-NCO; 2270 cm^{-1}) [5]. Figure 2 shows the FT-IR spectrum of one of the acrylate oligomers. The absorption bands at 3390, 1730, and 810 cm^{-1} correspond to stretching of the –NH, C=O, and C=C groups.

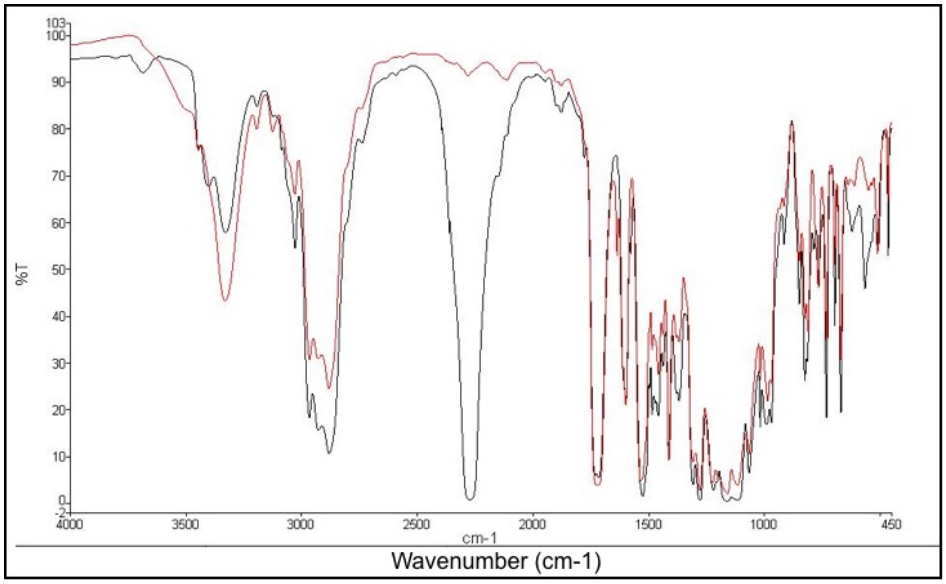

Figure 2: FT-IR spectra of a fluorinated urethane acrylate oligomer. The black trace is the stretching frequency analysis of the prepolymer before the isocyanate groups were end-capped with HEMA. The red trace indicates the final product with no remaining isocyanate groups at 2270 cm^{-1}.

The chemical structure of the diol component in each UA resin system was modified to adjust the refractive index. In particular, fluorine was introduced in different amounts to reduce the refractive index. We introduced fluorine groups in urethane structure by using fluorosurfactant diols (Figure 3). In addition to controlling the refractive index, there are several advantages for using the fluoro-surfactants in the structure of the urethane acrylate. i) They allow air release and de-aeration, which minimizes the formation of surface defects; ii) they act as flow and leveling agents, which improves the coating appearance and reduces the need for multiple additives, and iii) they are impermeable to water and impart chemical stability and weather resistance.

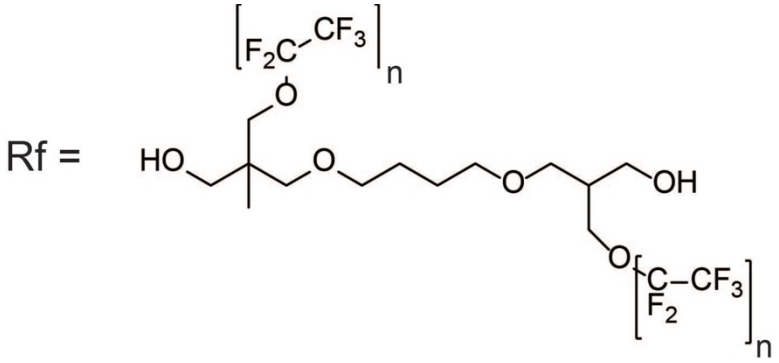

Figure 3: General structure of fluoro-surfactant diols used in the synthesis of the urethane acrylate resin systems. The molecular weight and fluorine content of these diols varied between oligomers.

Physical Characterization of the UA Films

UV-Curing. NanoSonic performed a series of thermal, mechanical, and environmental durability tests on cured films of the urethane acrylate polymer. Films of the UA resin were prepared by irradiation of the prepolymer under a UV light source shown in Figure 4. In the presence of UV light (λ = 365 nm) and a 5 wt% photoinitiator, the UA resin cured within 10 seconds.

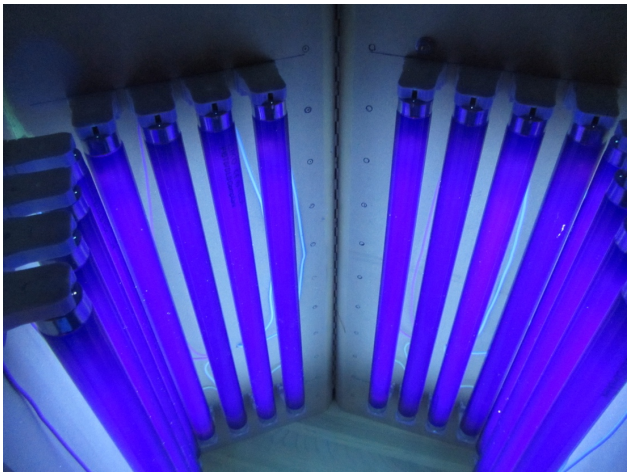

Figure 4: Side view of the UV chamber fabricated for curing the urethane acrylate prepolymer.

Thermal Performance. The thermal performance on the urethane acrylate system allowed us to determine temperature range at which the polymer system is operational. Thermal analysis was performed in-house using NanoSonic's TA Instruments thermogravimetric analyzer (TGA). TGA is a technique that monitors the mass of a material as a function of temperature. Thermal degradation is reported as the temperature at which the sample material looses 5% of its original mass value. The thermogravimetric (TG) analysis curves for three different urethane acrylate films (UA1-UA3) are shown in Figure 5. These films have different diol linker chemistries. The 5% weight loss value is between 240 and 270°C. The thermal decomposition begins with degradation of the side chains, followed by decomposition of the aromatic rings.

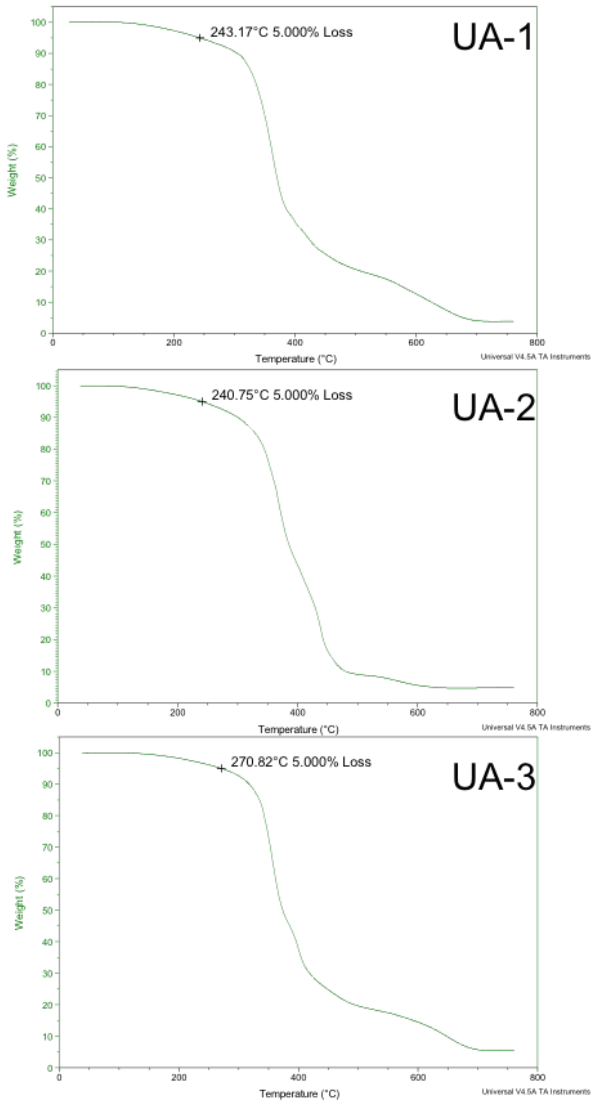

Figure 5: TGA thermograms of urethane acrylate (UA) films having different linker chemistries.

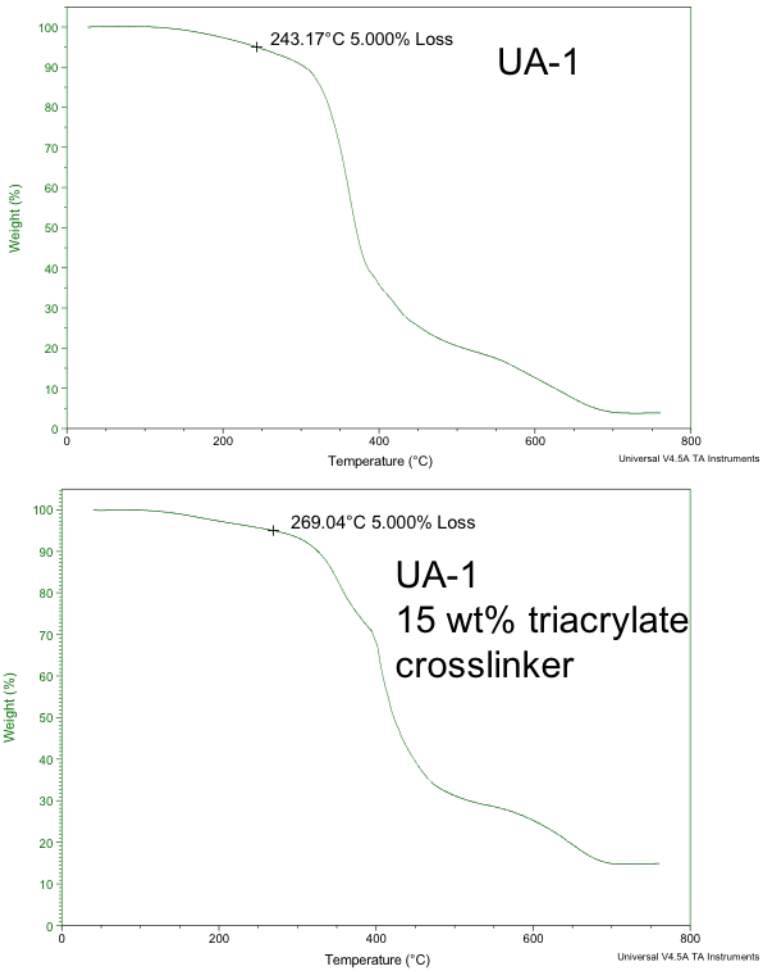

Figure 6: Thermogravimetric thermograms of UA1 with (*bottom*) and without (*top*) the addition of 15 wt% triacrylate crosslinker.

The incorporation of a triacrylate crosslinker increases the temperature at which 5% weight loss occurs from 243°C to 269°C (Figure 6).

Mechanical Properties. We measured the tensile strength, modulus, and elongation at break of free-standing films of the UA resin systems. NanoSonic performs mechanical testing with our bench-top 50kg capacity load frame (Figure 7) per ASTM D 638: *Standard Test Method for Tensile Properties of Plastics*. Three rectangular specimens are die cut (per ASTM D 638) from bulk material films and numbered; specimens are cut in two directions perpendicular to each other to confirm isentropic behavior within the material sample. The cross-sectional area of the test section for each of the rectangles are measured and recorded in the program that controls the load frame prior to testing. The specimens are then secured in the grips and pulled in tension to failure at a constant rate.

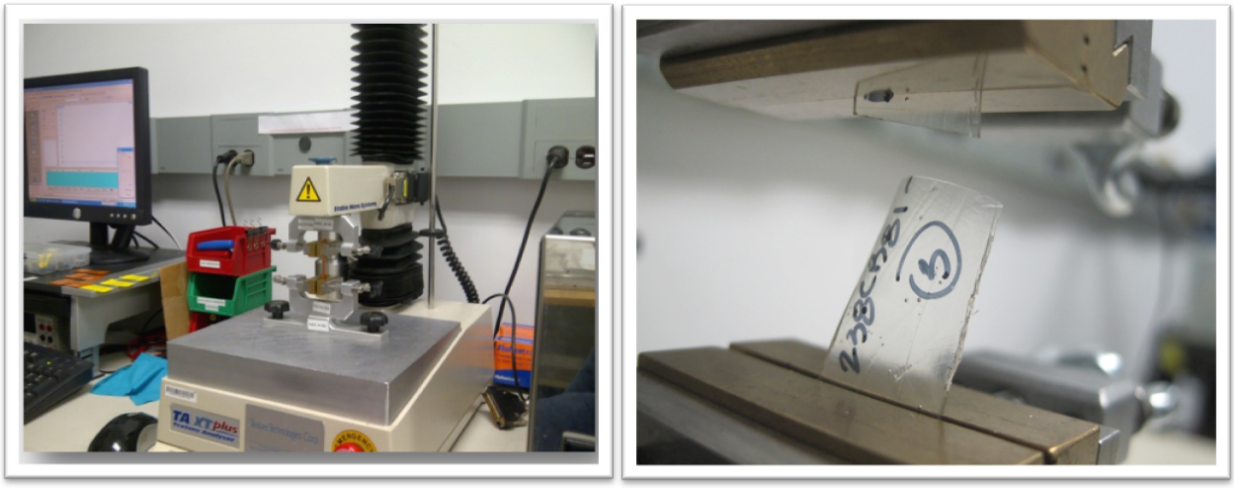

Figure 7: NanoSonic's Texture Analyzer bench-top load frame with 50kg capacity (*left*) and image of rectangular specimen after testing (*right*).

Each specimen was evaluated for peak stress, elongation at peak stress and Young's modulus of elasticity, and the results for the three rectangular specimens were averaged to provide an overall picture of the behavior of the materials tested. The results from these tests are tabulated in Table I, and an example of the stress-stress curve for one of the UA films is plotted in Figure 8.

Table I: Overview of the mechanical testing results performed on the UA films.

Sample ID	Avg. Modulus (MPa)	Elongation (%)	Avg. Stress (MPa)
238CB65	6.65	28.87	1.32
238CB73	11.69	50.68	2.46
238CB81_d	38.82	9.85	2.31
238CB83_2c	94.76	18.99	6.23

We increased the modulus of the films in 238CB81_d and 238CB83_2c by incorporating 15wt% tri-acrylate and tetra-acrylate crosslinking groups.

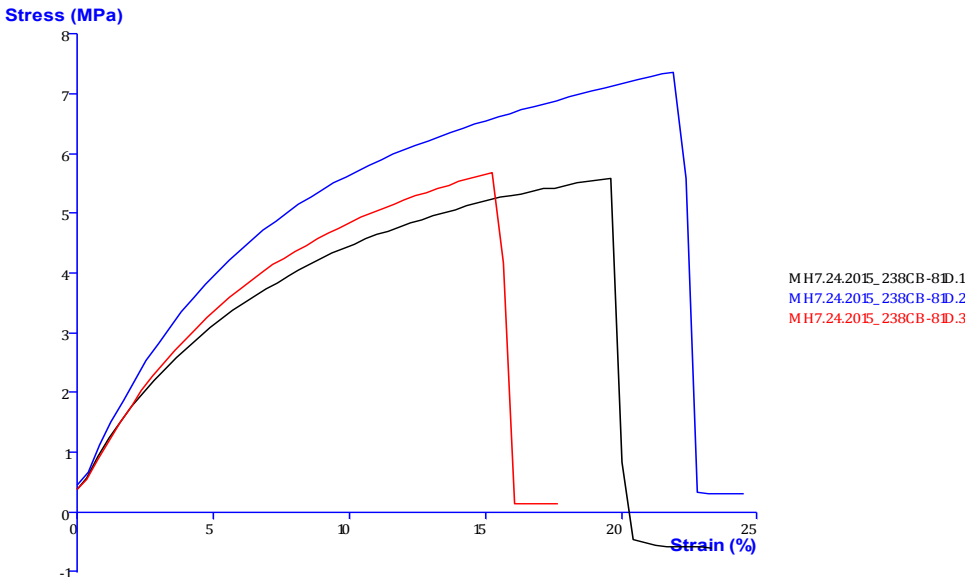

Figure 8: Stress-strain curves for tensile tests of one of the UA films.

Abrasion Evaluation. NanoSonic uses a Taber Abrader method and the Taber Abraser shown in Figure 9 to evaluate and optimize coatings with regard to their resistance to abrasion.

Figure 9: NanoSonic's Taber Abraser.

We performed this testing method using ASTM D 4060: Standard Test Method for Abrasion Resistance of Organic Coatings by the Taber Abraser. The sample films were abraded with C-10 wheels having 1,000 gram weights for 1,000 cycles. The samples were analyzed for mass loss and a wear index value—a measure of how well a system

resists abrasion—was calculated. The wear index is calculated using the following equation

$$WI = \frac{\Delta m * 1{,}000}{N} ,$$

where *WI* is the wear index, Δm is the mass difference in units of milligram and *N* is the number of cycles completed. NanoSonic uses this testing method to down-select optimal coatings having low *WI* values.

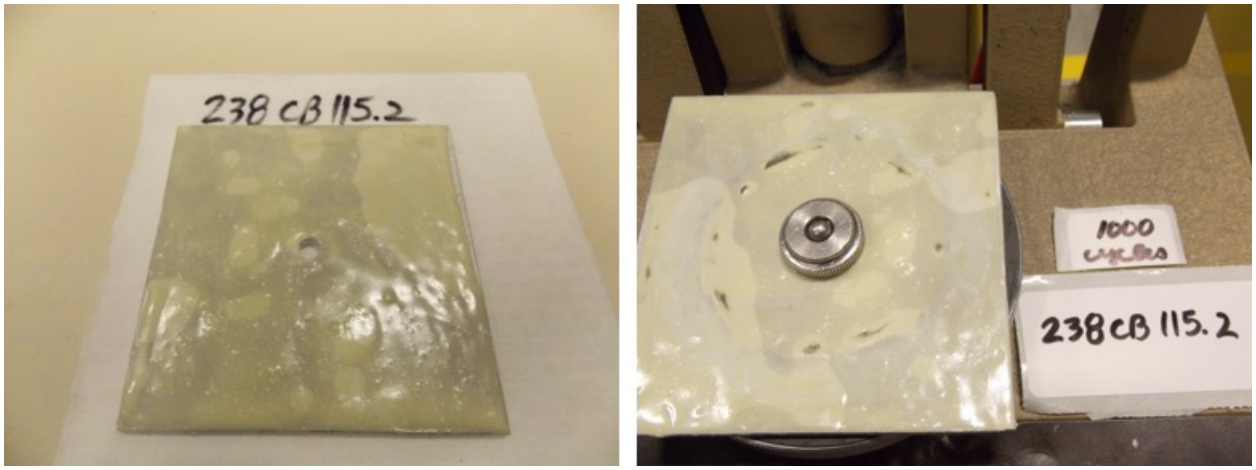

Figure 10. Aluminum coupon coated with fluorinated polyurethane acrylate resin. Image of sample immediately before abrasion analysis (*left*). Image of sample following 1,000 cycles (*right*). The wear index of this sample is 26.6.

As shown in Figure 10, the F-PUA coating deposited directly on aluminum, with no primer, showed excellent minimal weight loss with a *WI* of 26.6. For comparison, PSX-700, a polysiloxane coating used in both military and commercial applications, has a reported *WI* of 53.

Optical Characterization

We measured the refractive index at 589.3 nm using NanoSonic's Abbe Refractometer. As expected the refractive index decreased with an increase in the fluorine content in the series of synthesized urethane acrylate resins. As a control, we made a non-fluorinated urethane acrylate; this oligomer has the highest refractive index (1.5167). Table II summarizes these results.

Attenuation of 60dB/km has been estimated on 100m lengths of fiber fabricated during the reporting period. For short-distance jumper cables, this attenuation is negligible because total attenuation is dominated by connector insertion losses and not fiber attenuation.

Figure 11: NanoSonic's Abbe Refractometer.

Table II: Summary of the refractive indices measured for the synthesized polyurethane acrylate resins. The fluorine content increases from UA1 to UA5 and results in a corresponding decrease in the refractive index.

Fluorinated Urethane Acrylates	Refractive Index
UA1 (238CB104)	1.4220
UA2 (238CB70)	1.4640
UA3 (238CB129)	1.4780
UA4 (238CB73)	1.4855
UA5 (238CB79)	1.4965
Non-fluorinated Urethane Acrylate (238CB85)	1.5167

Composite Material for Optical Fiber Cladding

We investigated the use of micron-size fillers to improve the thermal and mechanical properties of the films, and to reduce weight and resin content. We introduced high-strength, low-density hollow glass microspheres (HGMs) as a filler in the urethane acrylate resin [6]. Hollow glass spheres are a promising inorganic filler with low density and low thermal conductivity since they consist of an outer stiff glass and an inner inert gas. To ensure that the HGMs have favorable surface interactions with the fluorinated UA matrix resin, we modified the surface of the spheres with perfluorinated alkylsilanes. We used a dilute hydrochloric acid solution (11 v/v% HCl in water) to hydroxylate the surface. After rinsing with water, we exposed the hydroxyl terminated glass spheres to a solution of perfluorinated alkylsilanes in toluene for 16 hours. We rinsed the surface functionalized spheres with water and isopropanol and dried with air. The surface morphology and elemental content was analyzed using scanning electron microscopy (SEM) and energy dispersive X-ray spectroscopy (EDS); results are shown in Figure 12.

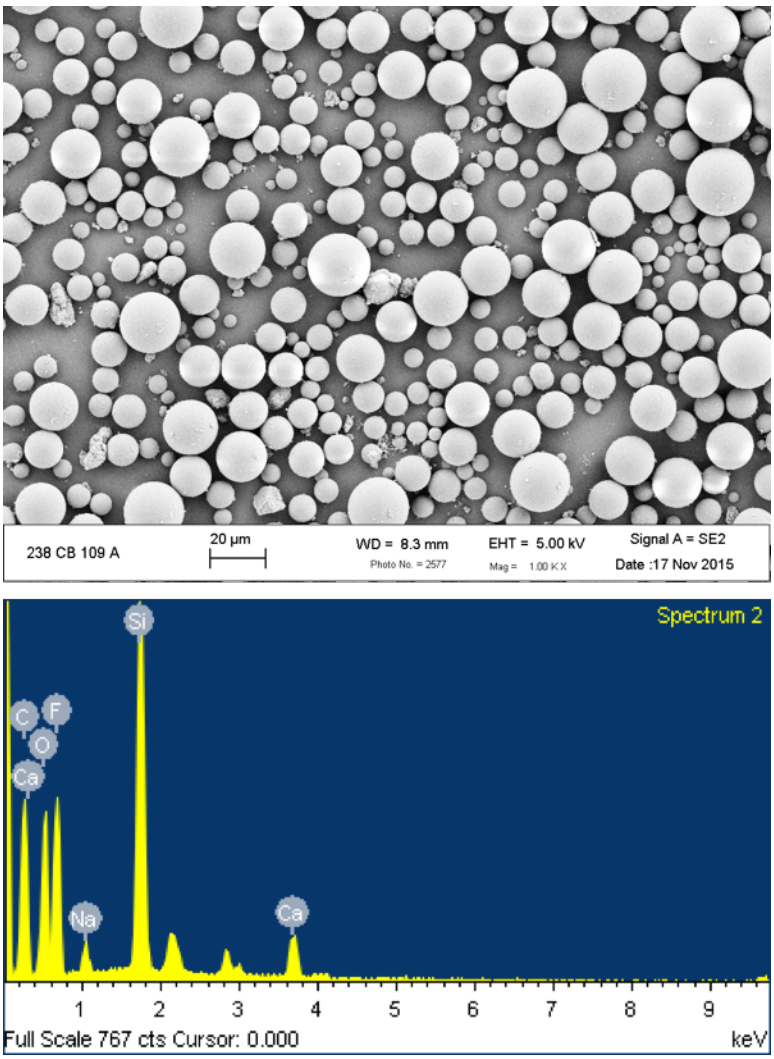

Figure 12: SEM of hollow glass microspheres (*top*) and EDS analysis (*bottom*) showing the elemental composition of the surface following exposure to fluorosilanes.

We introduced the F-terminated spheres to a UA resin system at a loading of 10 wt%; an SEM image of the resulting material is shown in Figure 13.

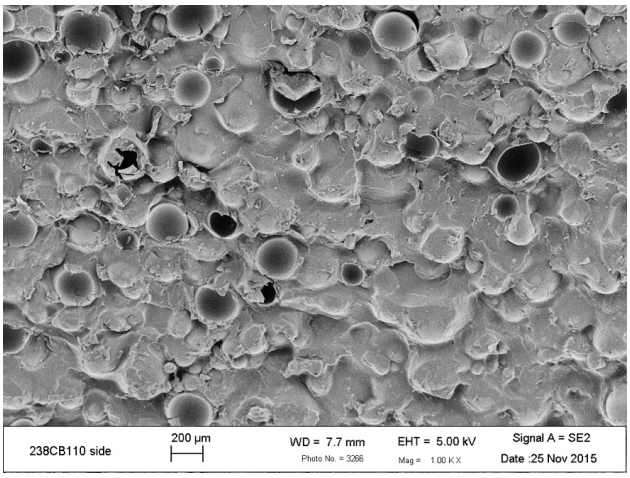

Figure 13: SEM analysis of a cross section of a UA resin filled with 10 wt% glass microspheres

The presence of the inorganic filler increased the temperature at which 5% weight loss occurs from 243°C to 320°C (Figure 14).

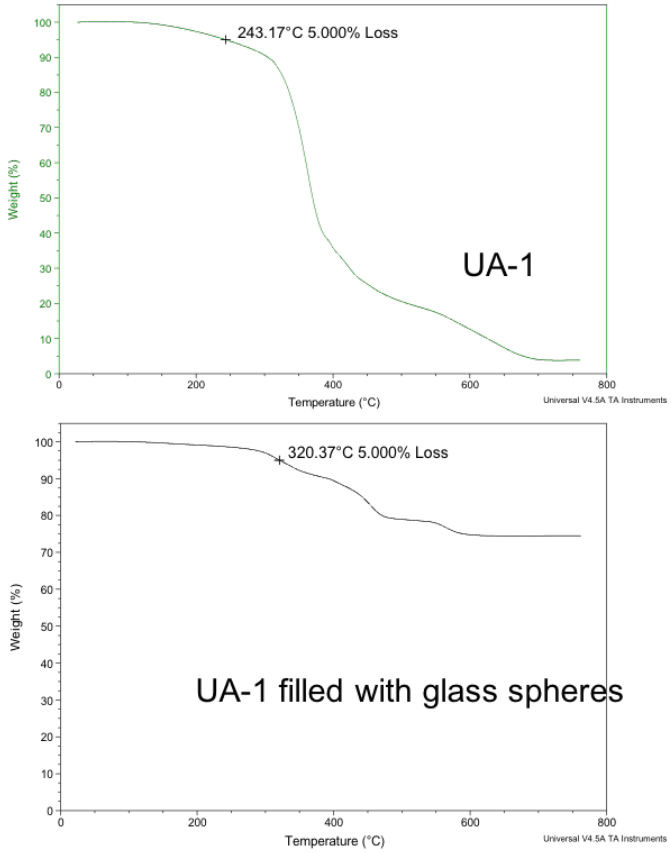

Figure 14: Thermograms of unfilled (*top*) and filled (*bottom*) UA films.

Figure 15 shows the current status of our polymer fiber draw tower system, located in one of our production labs.

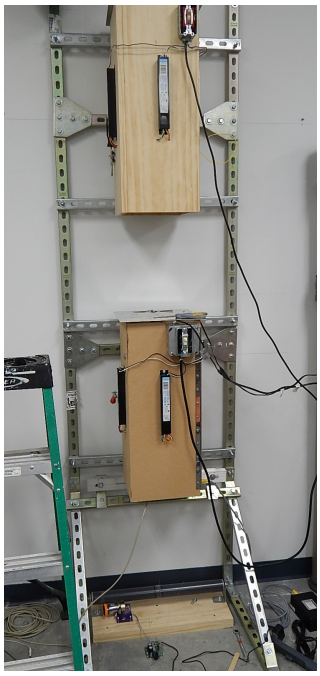

Figure 15: Polymer Fiber Draw Tower System.

Figure 16 shows GI-POF produced using this system and the self-assembly process demonstrated during Phase I. We have incorporated a dye into the outer jacketing layer of the fiber so it can be differentiated from other commercial fibers in the field.

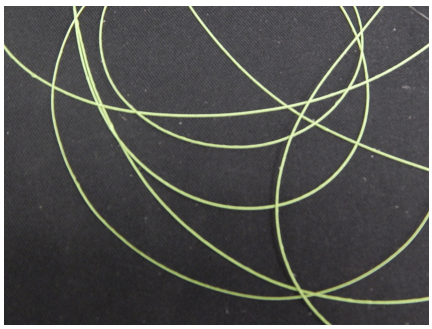

Figure 16: Green GI-POF Produced Using NanoSonic's Polymer Fiber Draw Tower System.

Figure 17 shows the results of this initial phase of work, specifically short jumper fibers made using the high and low index materials described above.

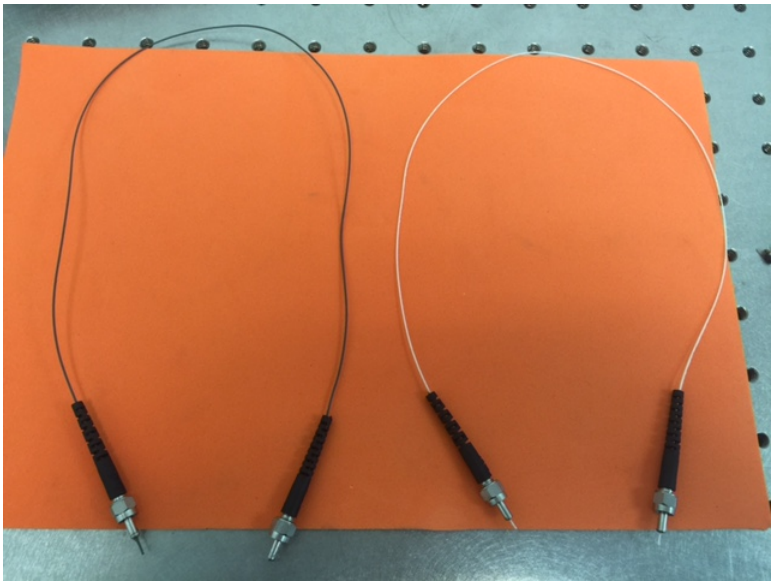

Figure 15: Samples of optical fiber coated two candidate thermal barrier coatings.

It was at this point in the Phase II program that United Technologies became interested in our self-assembly process and fiber materials, and visits were traded between United Technologies optical engineering staff and NanoSonic. Work on the Phase II program then focused on making fibers and materials for evaluation and testing by United Technologies; the Phase II PI was on-site for some of these tests at a United Technologies facility in nearby Ohio. Once the licensing agreement to United Technologies was completed, NanoSonic re-evaluated our program objectives and worked with Polymicro to outline fiber development tasks aimed at product sales but not in conflict with the UTC agreement. This work is summarized in Section II.B. that follows.

Accomplishment Section II.A. References

1. Kayaman-Apohan, N.; Demirici, R.; Cakir, M.; Gungor, A. UV-curable interpenetrating polymer networks based on acrylate/vinylether functionalized urethane oligomers. *Radiation Physics and Chemistry*, **2005**, *73*, 254-262.
2. Wang, F.; Hu, JQ.; Tu, W.P. Study on microstructure of UV-curable polyurethane acrylate films, *Progress in Organic Coatings*, **2008**, *62*, 245-250.
3. Moon, J.H.; Shul, Y.G.; Hong, S.Y.; Choi, Y.S.; Kim, H.T. A study on UV-curable adhesives for optical pick-up. International Journal of Adhesion and Adhesives, **2009**, *25*, 301-312.
4. Srivastava, A.; Agarwal, D.; Mistry, S.; Singh, J. UV curable polyurethane acrylate coatings for metal surfaces. Pigment and Resin Technology, 2008, 37, 217-223.
5. Bayramoglu, G.; Vezir, K.; Apohan, N.K.; Gungor, A. *Synthesis and characterization of UV curable dual hybrid oligomers based on epoxy acrylate*

containing pendant alkoxysilane groups. Progress in Organic Coatings, **2006**, *57*, 50-55.

6. Mutua, F.N.; Lin, P.; Koech, J.K.; Wang, Y. Surface Modification of Hollow Glass Microspheres. *Materials Science and Applications* **2012**, *3*, 856-860.

II.B. Addressing Molex/Polymicro Advanced Optical Fiber Product Needs

We nex focused on addressing Molex/Polymicro's indicated need for metal and high temperature coatings on specialized fibers as outlined in Section II.a., and specifically investigated the thermal and rheological properties of Ga_2O_3/GaIn as such a coating. Gallium-Indium (GaIn eutectic; 74.5% Ga, 25.5% In) is a liquid metal at room temperature (m.p. ~15.7°C) with metallic conductivity. This non-toxic liquid metal adheres readily to many surfaces, alloys with most metals, and disperses into polymer matrices.

Like many liquid metals, GaIn forms an oxide on its surface. This thin (~ 0.7 nm on average), electrically conducting, and self-passivating layer of oxide (Ga_2O_3) forms almost instantaneously upon exposure to air, or other oxygen containing environments. Ga_2O_3 has unique mechanical properties that facilities the formation of stable structures of Ga_2O_3/GaIn. For example, this liquid metal has been fabricated into sharp (~50 µm diameter) conical tips for use as non-damaging top electrodes that measure tunneling currents across thin organic films in the form of self-assembled monolayers (SAMs). Wires, drops, arches, antennas, and electrical interconnects have also been constructed from GaIn through injection in microchannels and through direct-write, three-dimensional (3D) printing. Figure 18 shows bare glass optical fibers obtained from Molex with test coatings of GaIn.

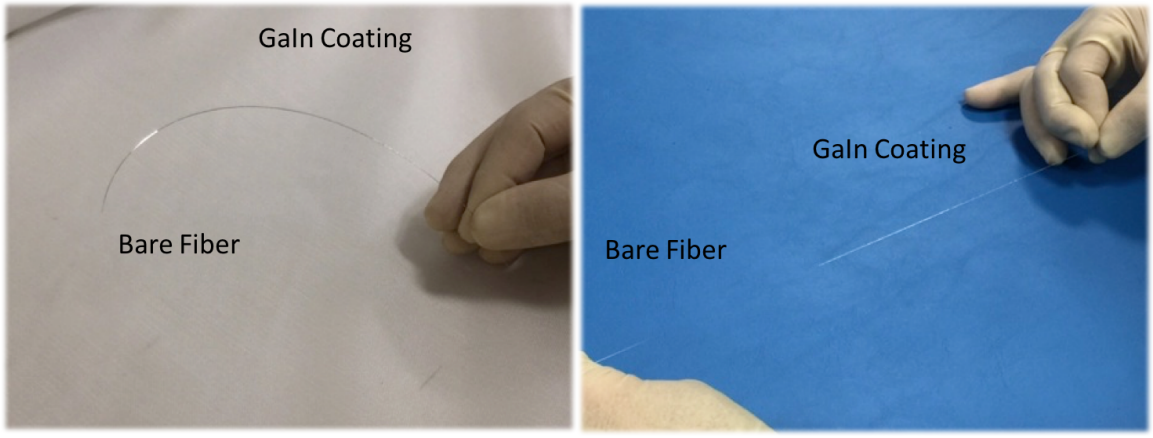

Figure 18: Coating of GaIn on Bare Glass Optical Fiber.

To begin to investigate the structure/property relationships of this material, we first analyzed the morphology of the Ga_2O_3 layer using Scanning Electron Microscopy (SEM) and investigated the elemental composition using Energy-Dispersive X-ray Spectroscopy (EDS). Results are shown in Figure 19 and indicate a smooth skin surface of the material, and that the atomic percentages of oxygen, gallium, and indium in the material are 5.7%, 75.9%, and 18.4%, respectively.

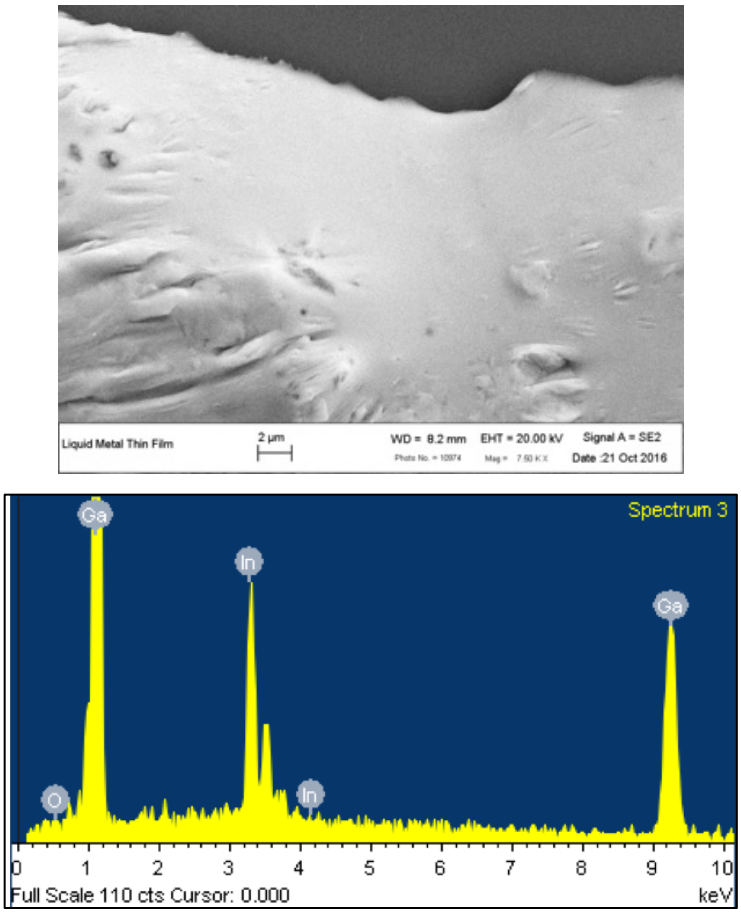

Figure 19: Scanning Electron Micrograph of Smooth Oxide Skin (top) and Elemental Composition (bottom) of Ga_2O_3/GaIn.

Next, we investigated the behavior of the liquid metal Ga_2O_3/GaIn as a function of increasing temperatures in air using Thermogravimetric Analysis (TGA). TGA determines the change in sample weight as a function of temperature or time. Using a TA Instruments TGA Q500, samples were evaluated for weight loss over a temperature range between 25˚C and 800˚C in air and at a heating rate of 20˚C/min.

Results are shown in Figure 20. We observed a slight increase (~0.4%) in the weight percent of the Ga_2O_3/GaIn sample with temperature, which is likely due to growth of the Ga_2O_3 layer. Other than a small increase in weight due to oxidation, we did not observe thermally-induced weight loss even after ~3 days of exposure to 800˚C. The thermal durability of the Ga_2O_3/GaIn, compared to coatings of standard organic polymer systems, makes it suitable for applications in high-temperature environments, as required by Molex.

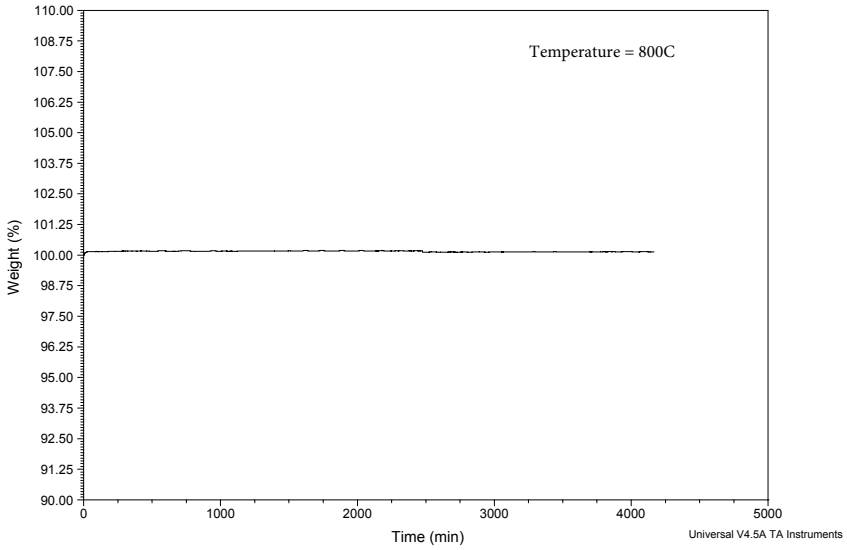

Figure 20: Thermal Decomposition Profile of Ga_2O_3/GaIn using Thermogravimetric Analysis. The Sample was Heated to a Temperature of 800˚C for ~3 Days.

Interestingly, structures of liquid metal Ga_2O_3/GaIn do not behave like classic liquids (for example, water), which continue to flow regardless of the force acting on them. Instead, the gallium oxide skin imparts resistance to flow. Due to the presence of an elastic oxide skin and a low-viscosity fluidic core, liquid metal Ga_2O_3/GaIn has been described as a viscoelastic material—meaning that it exhibits both viscous and elastic properties when undergoing deformation. The deformation response of Ga_2O_3/GaIn to an applied, controlled stress can be measured using a rheometer, thus enabling the characterization of the viscoelastic properties of both the oxide shell and the liquid GaIn core.

Accordingly, we analyzed the rheological properties of liquid Ga_2O_3/GaIn using a TA instruments AR2000EX stress-controlled rheometer equipped with stainless steel parallel plates that are 25 millimeters in diameter. Using this parallel plate geometry, the bottom plate is held stationary while the upper plate is rotated at a nominal speed v (m/s) that produces a controlled torque τ. Using a small syringe, we loaded the sample (0.49 milliliters) onto the stationary bottom plate and maintained a gap of 1000 µm between the top and bottom plates. For all rheological measurements, we analyzed a new sample of Ga_2O_3/GaIn, and did not perform pre-shear prior to testing. The measurements were performed at room temperature (25°C) and within 30 minutes of samples loading.

We first measured the viscosity η of Ga_2O_3/GaIn as a function of shear rate (s^{-1}). Values of viscosity measured with a rheometer are the ratio of the shearing stress to the shearing rate, according to equation 1.

$$\eta = \frac{shear\ stress\ \tau}{shear\ rate\ \gamma} = \frac{Pa}{s^{-1}} \quad \text{(eq. 1)}$$

Plotting the viscosity as a function of the shear rate produces a viscosity curve as shown in Figure 4. The viscosity of simple Newtonian materials (for example, water and mineral oil) are independent of shear rate. Many structured fluids, on the other hand, exhibit a strong decrease in viscosity as the shear rate increases. Shear forces can break the structure of materials, leading to a reduction in viscosity. Here, we observe a significant reduction in the viscosity of the liquid metal as the shear rate increases from 1E-3 s^{-1} to 1000 s^{-1}.

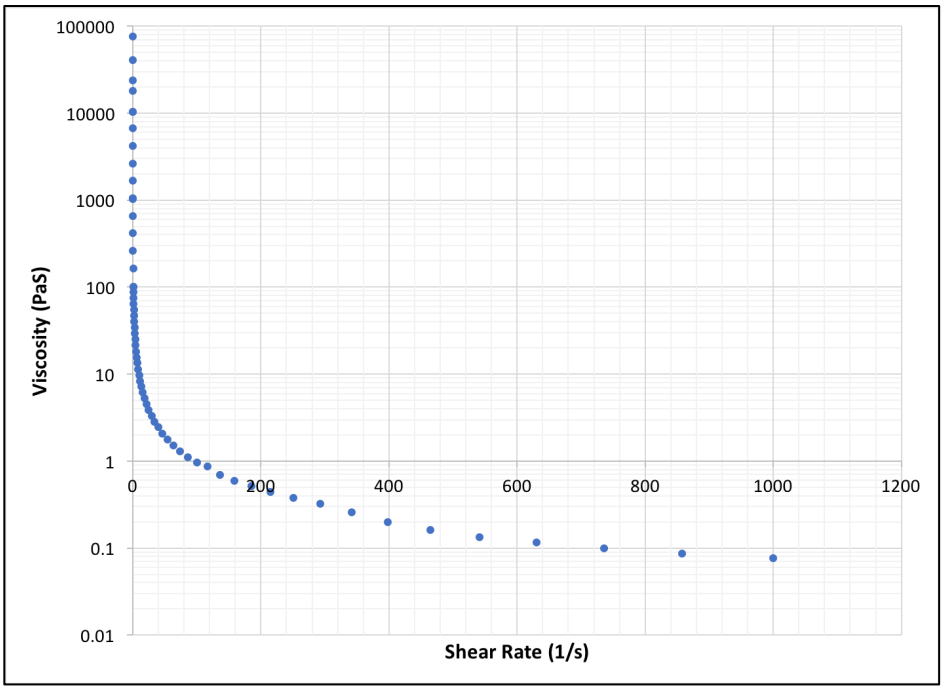

Figure 21: Viscosity Curve for Ga_2O_3/GaIn.

We also monitored the viscosity of Ga_2O_3/GaIn as a function of shear stress (Pa) using a continuous ramp method and increasing the torque τ (N-m) from 0 to 1000. Generally, structured fluids do not flow until a critical stress level has been reached, often called the yield stress. The stress at the viscosity maximum represents the yield stress value. The material exhibits elastic behavior below the yield stress value; exceeding the yield stress causes the structure of the material to break and flow.

Viscoelastic materials, such as liquid Ga_2O_3/GaIn, show pronounced viscosity maxima. Figure 22 shows a sharp viscosity maximum at a yield stress of ~29 Pa, or ~0.72 N/m. Prior to the yield point, the stress is stored elastically in the gallium oxide skin causing the material to resist flow.

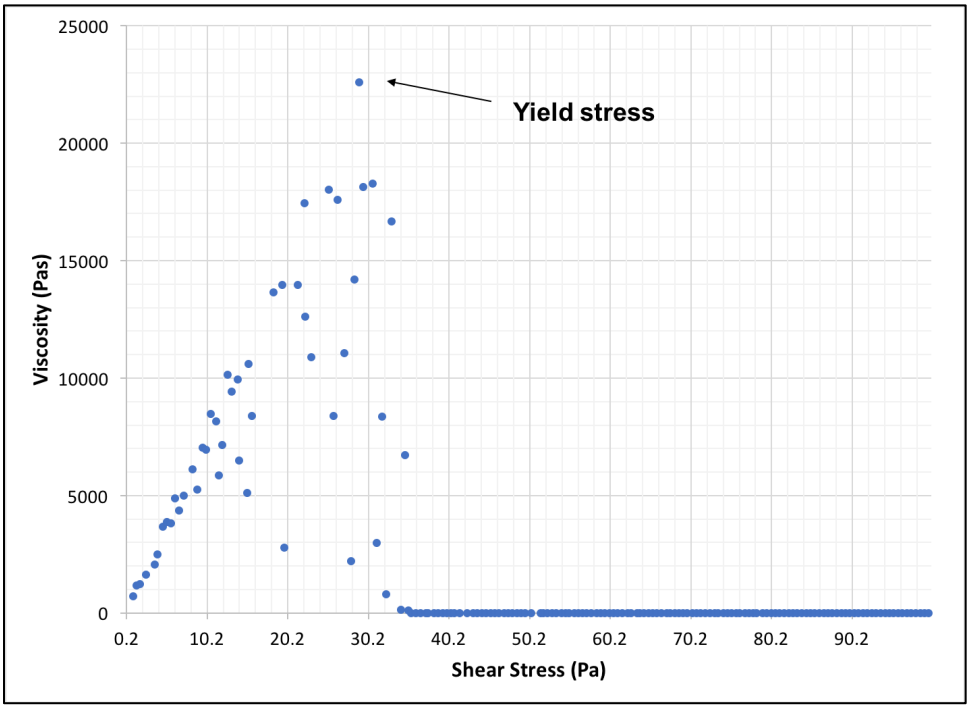

Figure 22: Yield Stress Measurement for Ga_2O_3/GaIn.

The rheological behavior of viscoelastic materials is typically independent of strain up to a critical strain level. Beyond the critical strain point, the material behaves non-linearly and the elastic storage modulus (G') and viscous modulus (G") begin to decline. We performed strain sweep measurements on Ga_2O_3/GaIn at an angular frequency of 6.283 rad/s. The torque required to oscillate the top plate sinusoidally, with a constant frequency ω (rad/s), is shown in equation 2.

$$\gamma_s = \frac{R\theta}{d} = \gamma_0 \sin(\omega t) \,, \qquad \text{(eq. 2)}$$

where *R* is the radius of the plate, d is the gap between the plates, t is time, γ_s is the surface strain, and γ_0 is the strain amplitude.

Figure 23 shows the results for the strain sweep measurement on Ga_2O_3/GaIn and summarizes the behavior of G' and G'' as a function of strain.

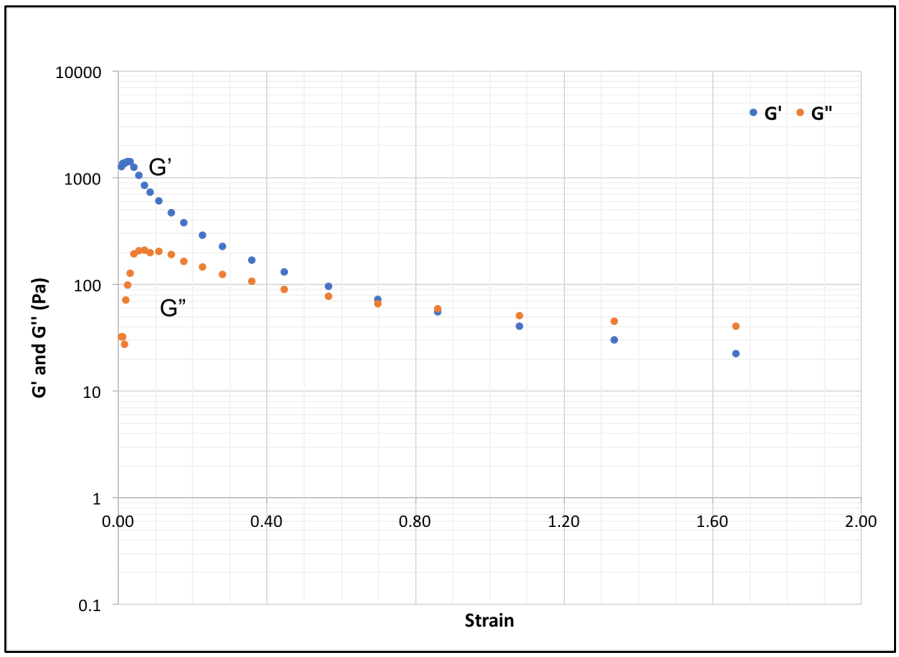

Figure 23: Viscoelastic Studies of Liquid Ga_2O_3/GaIn. G' and G" are Plotted as a Function of Strain.

According to the plot in Figure 23, the elastic modulus, G', of Ga_2O_3/GaIn is independent of applied strain at very low strains (below ~0.08). At strains below ~0.9, G' > G", indicating that the elastic behavior of the Ga_2O_3 dominates the rheological properties in the low strain region. After the elastic oxide skin begins to yield and break at increasing strains, the low-viscosity GaIn is able to flow and G" > G'.

Liquid Metal/Polymer Composite System

In addition to investigating Ga_2O_3/GaIn as thin optical fiber coating, we also dispersed the liquid metal at defined weight percentages into a custom siloxane polymer system (Figure 24). As a liquid metal, GaIn disperses readily into liquid pre-polymers, thereby making the metal-polymer composite processing steps straightforward. We are currently investigating this metal/polymer composite system as an additional optical fiber coating that may be easier for Polymicro to apply to fibers during the draw process using conventional polymer coating cups.

Figure 24: GaIn/Polymer Composite Systems. GaIn Liquid Metal was dispersed in NanoSonic's Custom Siloxane Polymer System at 14 (left) and 30 (right) Weight Percent.

GaIn/polymer composite resins of this type were delivered to Polymicro for coating on glass singlemode optical fiber and then tested for electrical conductivity and thermal properties. Results of this and other testing by Polymicro are summarized in Section II.D.

II.C. Polymer Fiber Jumpers, Hydrogen Non-permeable Fiber Coatings, High and Low Temperature Fiber Coatings

Prototype Fiber Jumper Production

NanoSonic produced test fibers using its unique materials and processing methods. Maximum production was on the order of 50 meters per week, typically using the different cladding and jacketing materials for the types of testing outlined previously. Several groups performed fiber and material testing. These groups were either subcontractors on the Phase II program (Virginia Tech and Molex) or established or potential licensees/customers/partners (United Technologies, Sikorsky, Schlumberger, Molex, which was both a subcontractor and potential licensee/customer, and by the Giles County, Virginia, school system).

Virginia Tech Fiber Jumper Evaluation

NanoSonic's Virginia Tech subcontractor operationally tested fabricated fiber jumpers in non-critical 1Gb/sec communication network paths in their on-campus information network. No failures or degradation of BER in comparison with conventional glass fiber jumpers were recorded over more than 10,000 hours (about 14 months) of continuous operation. Figure 25 shows NanoSonic prototype polymer fiber jumpers and their installation at Virginia Tech. The university is part of the GENI program, although the jumpers were installed or tested on GENI rack equipment due to Virginia Tech's perceived probability that the fibers might fail.

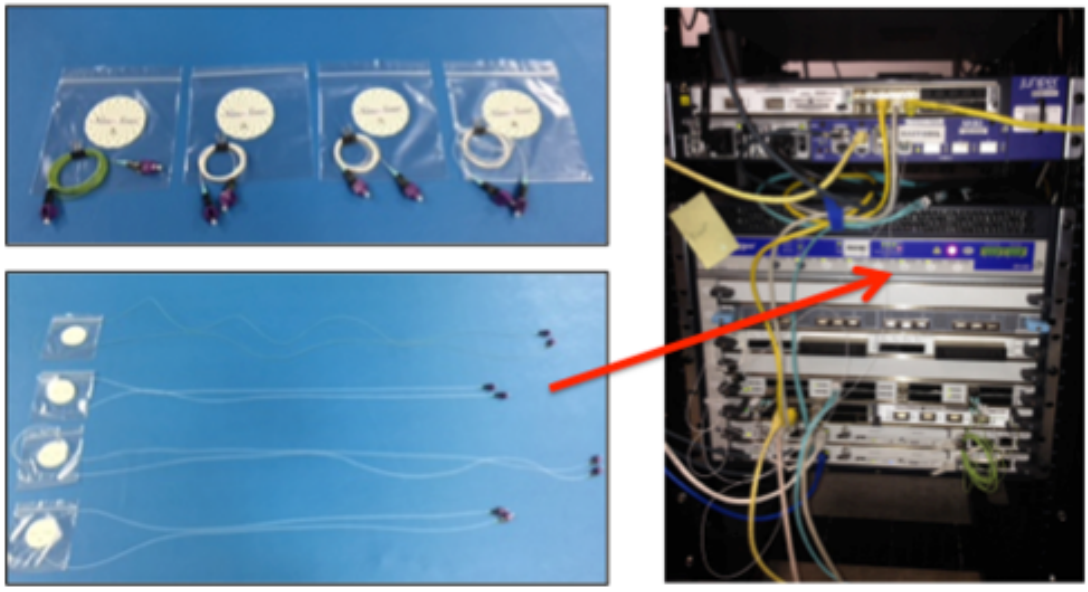

Figure 25: Virginia Tech Successful Testing of NanoSonic Fiber Jumpers.

Industry Testing of NanoSonic Fiber Jumpers

Test fibers and materials were sent to United Technology and Sikorsky for evaluation. The results of the United Technology testing were extensive and sufficiently positive that the company licensed the technology from NanoSonic. The results of testing by Sikorsky were not communicated to NanoSonic, although Sikorsky set up NanoSonic as a supplier through its supplier network so future sales and potential licensing are anticipated. NanoSonic visited Polymicro three times during the Phase II program, and hand delivered fibers and materials for their evaluation. We discussed possible licensing with Molex as well. No sample products were delivered to Schlumberger because they never specified downhole requirements. We are still defining the fields of use of all potential licensing opportunities to prevent overlap and complications.

It should be noted again and emphasized that Dawnbreaker Inc. was instrumental in setting up the framework for our license to United Technologies and for suggesting how additional non-overlapping licenses can be created with other companies. Pete Hunt at Dawnbreaker followed up with NanoSonic regularly by phone and email to discuss status and future directions. The PI met with Mr. Hunt twice during the Phase II program and to discuss current status and additional opportunities. Interaction with Dawnbreaker has been much more than we anticipated.

Low H_2 Permeability and Embrittlement

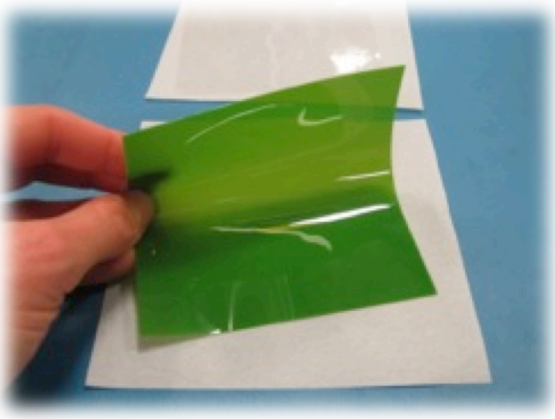

NanoSonic also addressed the additional technical goals outlined above. First, NanoSonic developed a series of low T_g polymer films for H_2 permeance testing per ASTM D 1434. A sample material is shown in the inset at right. A total of (3) 5” x 5” films were delivered per formulation, pre- and post- triple cold flex test (Figure 26) to Polyhedron Laboratories® in Houston, TX (Table III).

The primary interest in low hydrogen permeance coatings is as a way to lengthen the time that hydrogen-loaded fibers can be fabricated, shipped and stored prior to the writing of FBGs used to route specific wavelength signals in WDM and other systems. We worked on this with Molex. However, Dawnbreaker suggested that there may be significant other commercial opportunities for the same material. It is well known that stainless steel is susceptible to H_2 embrittlement; high-strength stainless steel becomes brittle and fractures upon exposure to H_2. Lone hydrogen atoms diffuse through the metal, recombine in the matrix voids to form H_2, and create an internal pressure increase that leads to reduced ductility and tensile strength, and localized defect sites,

causing the metal to crack. Ferrosilicates are one material used to treat metals to prevent this type of failure.

NanoSonic has developed a low H_2 permeance polymer matrix resin based on the same basic chemistry as the outer jacketing of our fibers. Additional tests for H_2 embrittlement include ASTM F1459-06 and G142-98 were conducted outside the DOE Phase II program, and through NanoSonic's Internal R&D (IRAD) program. H_2 permeance, solubility, and diffusion are each important to understanding the potential for embrittlement.

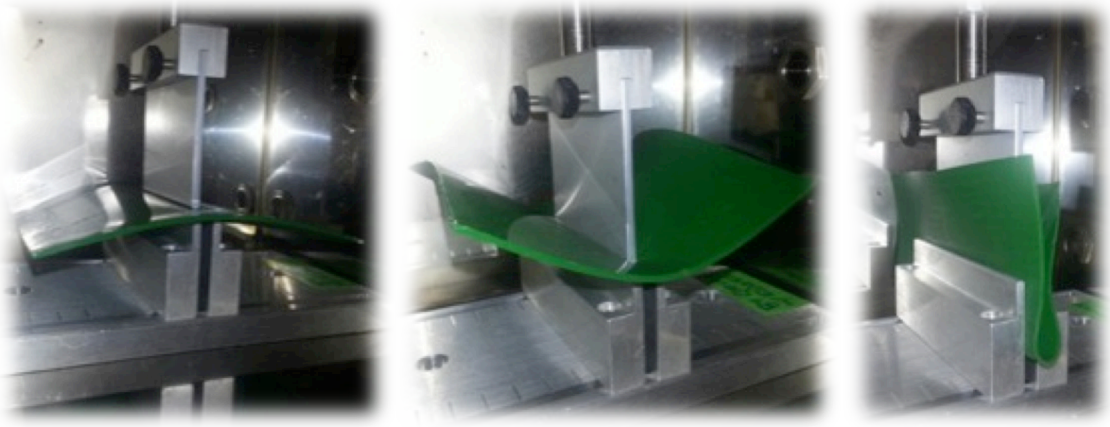

Figure 26: NanoSonic Triple Cold Flex Test for H_2 Permeance Specimens Conducted at -50 °C on Base Film: Shown Flat, Mid-Way, and at 180 ° Fold.

Table III: Ultra Low H_2 Permeance, 0.31 cc/100in^2•Atm•day Post- Cold Flex.

Hydrogen Permeance by ASTM D 1434

Sample No.	Thickness (in)	Hydrogen Permeance (cc/ 100in^2·Atm·day)
Set 4 - Lot # LB199-119		
Hydrogen - 10A, 10B, 10C	0.01060	0.29 0.22 0.20 AV = 0.24 ± 0.04
Hydrogen Cold - 10A, 10B, 10C	0.01100	0.36 0.35 0.20 AV = 0.31 ± 0.09

Low T_g, Fiber Materials for Low Temperature Flexibility

NanoSonic also designed a series of materials based on thermoset (cross-linked) high performance, unsaturated polyorganosiloxanes with a UV package to mitigate ozone and UV degradation of importance to future Molex optical fiber products. These polymers were synthesized and purified in-house, and evaluated at nearby Virginia Tech using gas chromatography to verify that all residual monomers are removed – to prevent offgassing and leaching. Non-proprietary constituents of the base material include the following.

1. siloxane backbone – to meet the requisite low T_g for cryogenic flexibility (Figure 27 which shows a measured very low T_g = -100°C)
2. urethane component – amine bonding to reinforcing agents
3. fluorinated siloxane – weatherability against UV, ozone, and atomic oxygen (AO)
4. fluorinated urethane – adhesion to PE heat seaming,
5. tailored molecular weight (M_n) - for processability with extrusion manufacturing

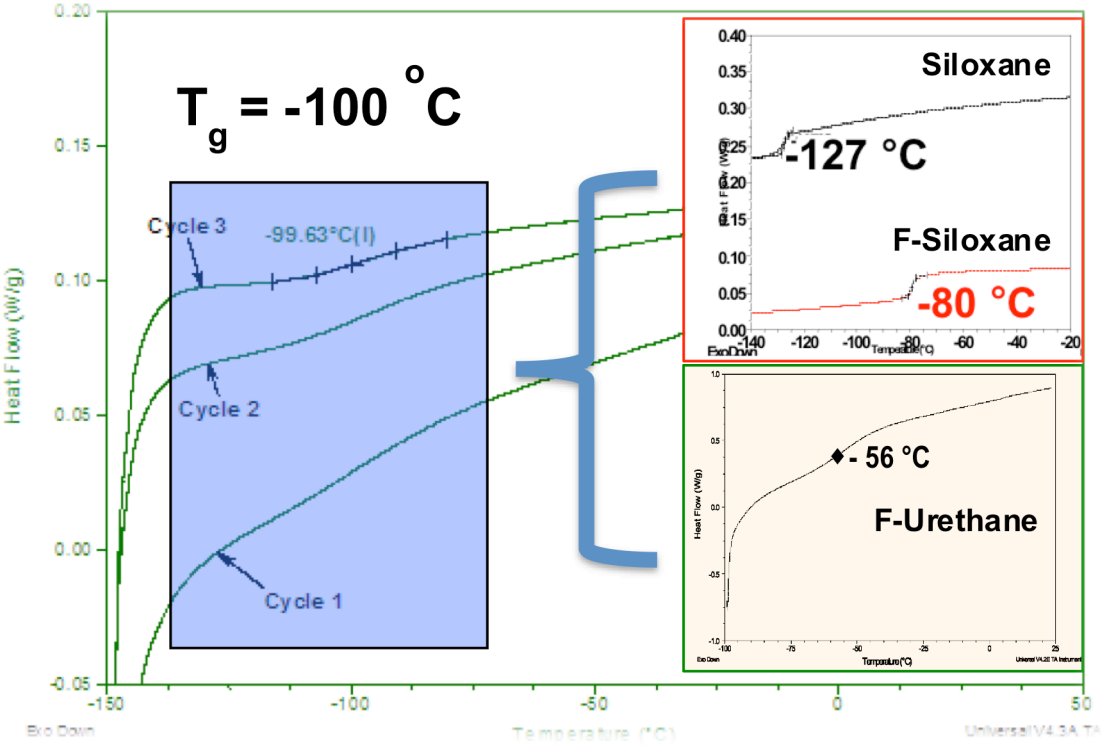

Figure 27: Ultra Low T_g Poly(organosiloxanes) Base Materials.

Materials of this type were delivered to Polymicro for testing.

Design and Development of High-Temperature Thermal Barrier Coatings for Optical Fiber

We have also addressed Molex' concern about high temperature coatings for polymer fibers. The application of optical fiber in aggressive environments may lead to degradation of performance, and thus poor reliability installed. Therefore, the conservation of the physical characteristics in harsh environments is critical to assure good performance over long periods. An appropriately designed coating on optical fiber can provide protection against extrinsic factors that may compromise strength and performance.

We designed and tested coatings to increase the thermal durability of the polymer optical fibers in extreme temperature environments. These coatings are applied directly on the cladding of the optical fiber.

Nanocomposite Systems as Thermal Barrier Coatings. We evaluated micron size particles as fillers to reduce the thermal conductivity, so increase the high temperature performance, of the polymer coatings. These nanocomposite coatings do not interfere with the propagation of the electromagnetic waves since it is applied external to the fiber cladding.

We tested the thermal performance of the coatings by measuring the thermal knockdown temperature of the coating. The thermal knockdown is the reduction in temperature of the substrate that is imparted by the coating.

To evaluate thermal knockdown, we applied the coating to a 4" x 4" glass substrate. We mounted the sample vertically with a 2" offset from the tip of a heat gun set at 400°F and qualitative fan speed of 4 bars (Figure 28). Type J thermocouples with adhesive backing were attached approximately to the center of the front side of the sample facing the heat source and the backside of the substrate. Measurements were taken at a sampling rate of 5 seconds for a period of 5 minutes. An uncoated glass substrate was also measured as the control.

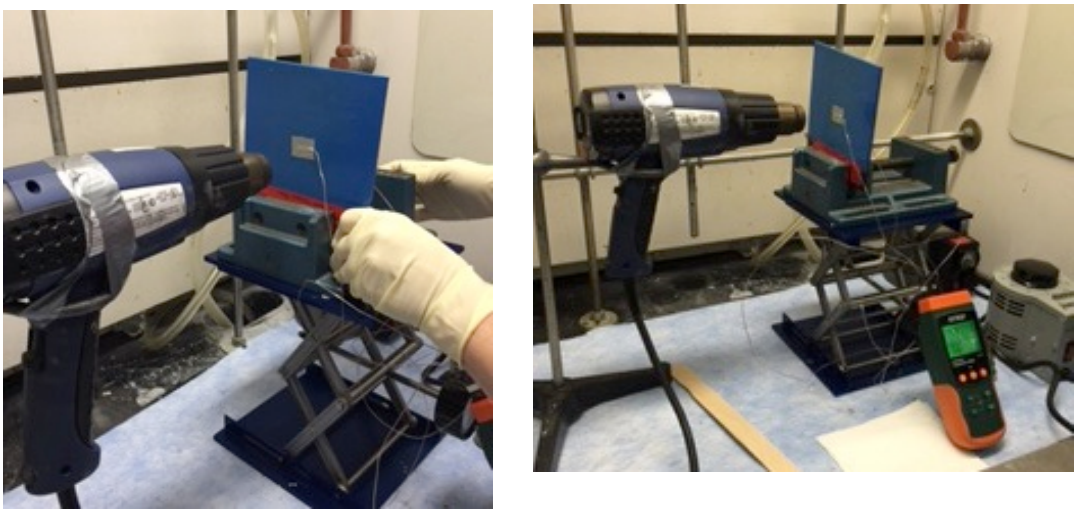

Figure 28: Set-up and Measurement of the Thermal Knockdown Imparted by NanoSonic's Coated Substrates.

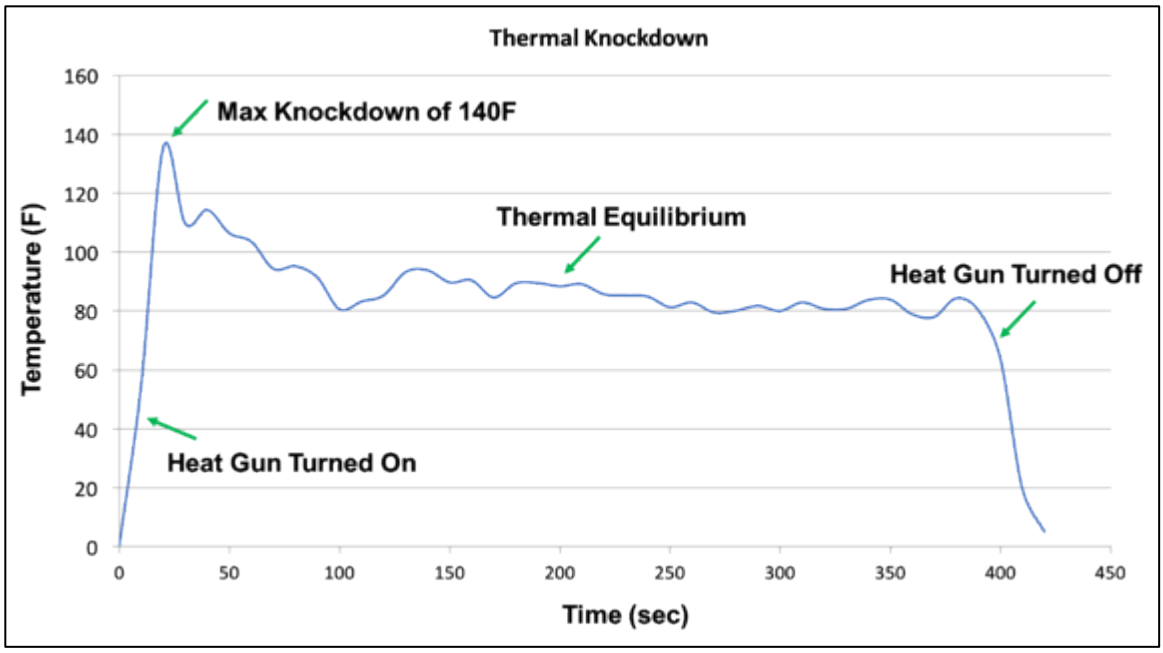

Figure 29: Thermal Knockdown Performance of Coating for Thermally Durable Polymer Optical Fiber.

We achieved at maximum thermal knockdown of 140°F. After ~50 seconds, the sample reaches thermal equilibrium (Figure 29).

Application of Thermal Barrier Coatings to Polymer Optical Fiber

Prior to sending test materials to Polymicro, we coated fabricated polymer optical fiber with the thermal barrier coating using the coating system that was designed and built in-house. The coating system is modified with a UV lighting system to enable the rapid (~20 seconds) cure of the thermal barrier coating on the fiber, this corresponds approximately to processing conditions at Polymicro. Figure 30 shows the fiber partially coating with a green thermal barrier coating resin. We monitor and control the thickness of the coating using a non-contact system from BETA LaserMike. This high precision system enables diameter measurements with sub-micron accuracy.

Figure 30: Application of Thermal Barrier Coating to Polymer Optical Fiber (left). Monitoring Coating Thickness using Beta LaserMike Non-Contact Measurement System.

Polyimide Resin Systems as Ultra-High Temperature Coatings. We also developed ultra-high temperature, UV curable polyimide coatings as shown in Figure 31. This all polymer system has a high 5% weight loss value of ~438°C (820°F), meaning that it can be used in environments up to ~438°C (Figure 32) before its chemical structure begins to degrade. This material exceeds the 350-400°C goal specified by Polymicro and is a potential NanoSonic product.

Figure 31: Custom Synthesis of Ultra-High Temperature, UV-Curable Polyimide Resin System.

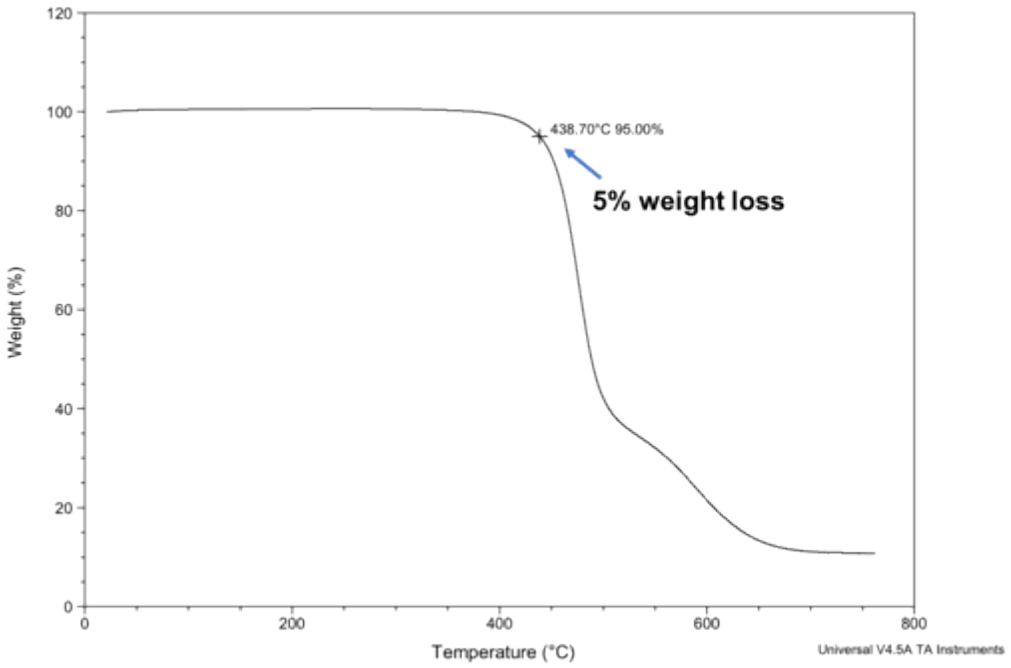

Figure 32: Thermogravimetric Analysis (TGA) of Ultra-High Temperature Polyimides for use as Optical Fiber Coatings in Extreme Temperature Environments.

Testing results are discussed in the results section II.D.

II.D. Final Polymicro Testing and Quantized Electron Propagation Summary

The DOE granted NanoSonic a no-cost time extension of the Phase II program to enable Polymicro to complete final testing on fiber materials sent to them for evaluation. During this period the funding per month on the program was low but there was sufficient time to revisit observations made during the Phase I program of quantized and partial quantized electron transfer in one-dimensional metal waveguides. Both of these issues are summarized in this section.

Polymicro Testing Results

NanoSonic worked with Polymicro materials engineers during on-site meetings and through correspondence to design the multiple optical fiber materials discussed in prior sections of this report. NanoSonic then experimentally synthesized materials and reported testing results to Polymicro for analysis. The four materials developed were

1. GaIn high temperature metal coating that could serve as a replacement for gold or aluminum currently deposited on glass fiber by Polymicro,
2. Hydrogen impermeable polymer coatings to inhibit the escape of hydrogen from loaded glass fibers used to manufacture FBGs,
3. Low glass transition temperature coatings, and
4. High temperature coatings.

Polymicro's laboratory work involved two primary steps. The first was to use the materials to coat flat glass substrates and observe their coating and curing properties. This was done with the first, second and fourth materials listed above. It was determined that there was a lower need for low glass temperature coatings that originally estimated so no further work was done with these coating materials.

Second was to use the materials to coat fibers on one of Polymicro's glass fiber draw towers during the draw process. This involved determining how the coating materials could be held and heated in a pressurized coating cup near the top of the tower and cured during draw. GaIn materials do not need to be cured as they solidify upon exposure to air and lower temperature. The cure kinetics studies that NanoSonic performed on the second and fourth materials were useful in estimating beginning cure routes during draw, specifically the required UV intensity and dwell time as the coated fiber passes the UV bulbs.

For the GaIn materials it was noted that bending the fiber caused the coating to rupture and reform. This is anticipated from experiments performed at NanoSonic with the fibers shown in Figure 18. The GaIn ruptures as the fiber is bent, then quickly reforms and holds the fiber in its bent shape. The result of this work has been that such coatings on glass fibers are probably not useful, but the use of similar materials in Molex' line of metal connectors may have merit. Molex identified individuals in their broader

connector business who may be able to use this technology. Connectors that re-connect after being stressed would potentially have a commercial market.

The hydrogen impermeable coatings were also successfully applied to glass fibers, and the long term testing of the hydrogen content of coated fibers as a function of time is ongoing. Ideally, hydrogen-loaded fibers could be coated and stored for an extended period of time prior to FBG writing; a shelf life of two years would be desirable. From initial data and Fick's Law calculations, we were able estimate that at the approximately 0.3 cc/100 in^2•Atm•day permeance for 250 micron-thick fiber coatings, the stored hydrogen concentration would decrease to 90% of its original value in about 17 months, which is close to the desired shelf life target. NanoSonic has shipped additional low permeance coating material to Polymicro and at the conclusion of the Phase II program is discussing the possible exclusive sale or licensing of materials to Molex.

The high temperature coating materials have also been evaluated on glass optical fibers although a separate application has developed that may supersede our interaction with Polymicro. A division of Lockheed Martin is interested in purchasing or potentially exclusively licensing the material from us, and an agreement may be reached with them prior to one with Polymicro. Lockheed Martin engineers from that group have visited us at NanoSonic twice during the past few months and while they have been onsite we have applied coatings to substrates, cured them and measured their properties. At this time we anticipate a large order for materials from that group.

Beyond the end of the Phase II program, NanoSonic anticipates continued work with Polymicro through our Independent Research And Development (IRAD) program. Although as a small company our IRAD program is not large, it is sufficient to provide the equivalent of a half time engineer to synthesize and evaluate materials in the lab.

Quantized and Partial Quantized Electron Propagation

During the Phase I DOE program, NanoSonic observed quantized electron propagation effects in materials and reported them in DOE reports. At the conclusion of the Phase II program, we collected our measurement information concerning these observations and they are outlined below. Important to future high-density computer and communication system hardware, they suggest methods to fabricate one-dimensional electron waveguides analogous to singlemode optical fiber. In these waveguides, ballistic electron propagation occurs, meaning that electron collisions with the material does not occur so heat is not generated. This has implications for low heat generating logic gates and memory devices. It should be noted that no time other than that required to arrange this report was spent on experimental work in this area.

NanoSonic and colleagues at Virginia Tech have investigated memristor devices through prior basic research.[1] Initial work involved making and testing simple metal-insulator-metal (MIM) memristor devices operated as memory structures and observing their data writing and erasing behaviors and switching characteristics at large bias voltages and currents. These are typically termed resistive random access memory (RRAM) devices. An ideal I/V curve of a unipolar RRAM device is sketched in Figure 33. Here a bias voltage of one or several volts is applied to create a resistive bridge between the top and bottom metal electrodes and perform the "WRITE" operation. Once the bridge is formed and data is stored, if the bias voltage is removed, the bridge remains intact. Reversing the bias voltage destroys the bridge and erases the data. However, if we look more carefully at the data write operation, we have seen the type of behavior shown in the measurement in Figure 34. Figure 35 shows detail of this quantum effect-based turn-on behavior.

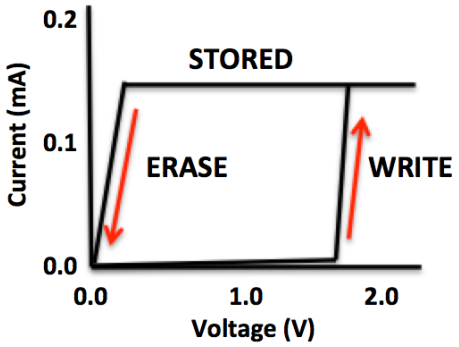

Figure 33: Ideal I/V Characteristic Curve for Unipolar MIM RRAM Device.

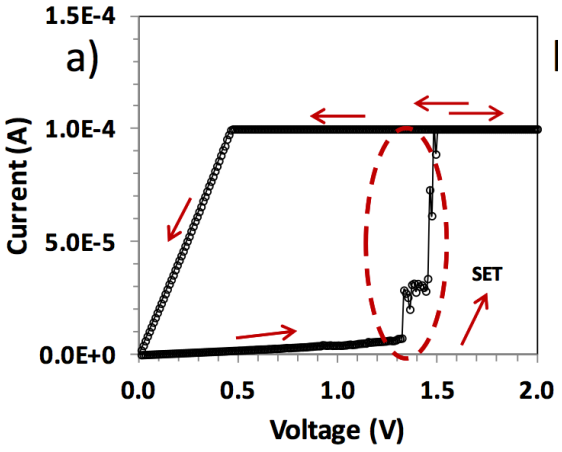

Figure 34: NanoSonic's Experimental Observation of WRITE/ERASE Operation of RRAM Test Device.

[1] Y. Kang (NanoSonic researcher), "Mechanisms, Conditions and Applications of Filament Formation and Rupture in Resistive Memories," Ph.D. dissertation, Virginia Tech, 2015.

Figure 35 shows one of our experimental measurements of the characteristic curve of one of our MIM RRAM devices that uses copper as the active metal electrode. Here, the vertical axis is shown as device conductance rather than current. Important is the turn-on effect seen during the WRITE or SET operation, at a bias voltage of about 1.4V. As we discuss below, this effect is due to the formation of a nanofilament bridge across the insulating layer in the structure, and provides a way to improve device performance. The measurement shown at left shows quantized conductance steps in the characteristic curve, meaning that as the device turns on, individual electron wavefunctions are progressively involved. Here the quantum conductance $G_0 = 2e^2/h$ is the first mode, $2G_0$ is the second mode and so on, where e is the electron charge and h is Planck's constant. Perhaps more interesting is the data shown at the right that exhibits partial quantized conductance steps.

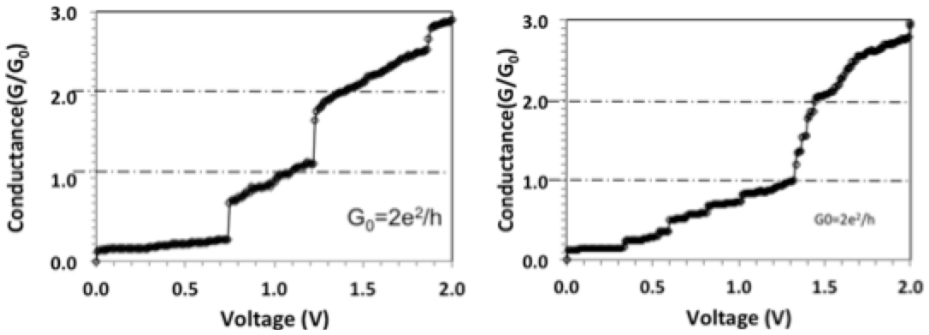

Figure 35: Observed Quantized Conductance Only (left), and Quantized and Partial Quantized Conductance (Right) in Graphene-Based MIM Structures.[2]

It should be noted that the slope of the steps shown in the plot at the left are due to the resistance of the probe leads to our Keithley semiconductor device analyzer and the resistance of the material. Between 0 and $1G_0$ in the plot at the right are shown five discrete steps of approximately 0.2 G_0 each. Important is that these measurements were made at room temperature and not at 4°K. The observations suggest that RRAM devices may be turned on at low conductance levels, on the order of $1G_0$ instead of the $20\text{-}30G_0$ at which conventional RRAM is operated. This means a potential reduction in bias current of as much as an order of magnitude, and a corresponding large reduction in dissipated power.

Related quantum effects have been considered analytically for more than 30 years. Daniel Tsui at Bell Labs predicted underlying concepts theoretically in 1982, for which he and others won the Nobel Prize in Physics in 1998. The quantized conductance is likely due to the nanofilament in the RRAM forming a one dimensional (1-D) electron waveguide at the exact time that the filament grows and just bridges the two electrodes; macroscopic large voltage/large current biasing overlooks this important "nanoeffect." The 1-D waveguide then poses geometrical and material boundary conditions on electron propagation. The solution to the propagation equation subject to these boundary conditions results in quantized propagation modes. The quantum

conductance $G_0 = 2e^2/h$ observed is the first of these modes; $2G_0$ is the second mode, and so on.

Our prior work also extended our initial observation of these effects in graphene-based MIM structures to similar observations in copper/oxide/platinum MIM devices in which copper nanodendrites form the conducting channel. These results were significant for two reasons - first because they show that such effects can occur in multiple material systems, and second because copper, unlike graphene, is commonly used in current semiconductor device manufacturing systems so should be easier to incorporate into Honeywell rad-hard memory manufacturing.

Model of Nanofilament-Based MIM RRAM Device

Our simple model of a nanofilament-based MIM RRAM device is shown in Figure 36. Corresponding to some of our prior experimental measurements, the top active electrode shown here is assumed to be copper; the copper is 'active' because with the application of an applied potential difference, copper ions migrate through the insulating oxide layer. The middle insulator layer is tantalum oxide, and the bottom inactive layer is platinum.

The model starts by assuming the application of a potential difference between the top and bottom electrodes as shown at the left. In response to the potential difference, the electrochemically active metal electrode material is oxidized. Because the insulating layer is very thin, the electric field (E=V/d) in the material is high, so mobile Cu^+ cations move through the insulator due to drift as well as diffusion. At the inert Pt counter electrode, these copper cations are reduced and create copper dendrites that gradually accumulate to form a highly conductive nanofilament that grows until it connects to the top copper electrode. Exactly at the point where connection between the filament and the electrode occurs, conduction between the electrodes and across the filament is through a very small diameter cross-section of the filament, presumably one atom or several atoms wide. Our model is that this situation corresponds to our observation of quantized conductance behavior, because at that point electrons are transported along a narrow constricted path that may be modeled as a local 1-D electron waveguide that interconnects the bulk top and bottom electrodes.

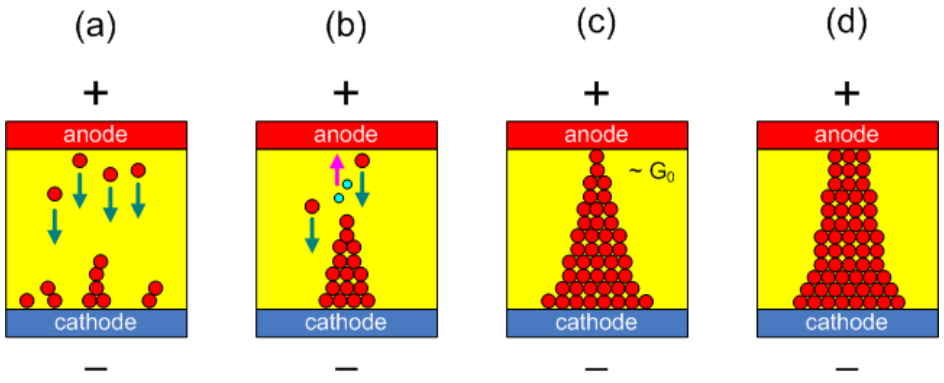

Figure 36: Model of the physical mechanisms of cation transport and nanofilament formation between active and inert electrodes separated by a thin insulator. Red circles represent Cu atoms and cations. Blue circles represent electrons. The yellow region represents the solid insulating electrolyte. The "+" and "-" signs indicate the voltage polarity relative to 0 V.

If the bias voltage is gradually increased beyond this initial attachment point shown in diagram (c) in Figure 36, the diameter of the filament grows, so the diameter of the attachment between the filament and the top electrode increases as shown in diagram (d), and the number of electrons transmitted through this larger area also increases. For this situation, bulk electron transport effectively occurs, so it is not possible to observe partial quantized conductance effects, only the ensemble average effect of many independent channels. This situation of bulk electron transport is what controls currently manufactured RRAM devices, and is what can be improved to reduce device power.

The status of our understanding of this basic research of memristor memory device results may thus be summarized as follows.

1. Quantized and partial quantized conductance effects may be observed, at room temperature, in MIM material systems based on copper nanofilaments as well as filaments of graphene nanoplatelets. This is important because copper is commonly used in current semiconductor processing so may allow adoption in IC manufacturing.
2. The MIM device construction allows us to study quantized and partial quantized conductance effects in ICs.
3. The charge transport mechanism in MIM structures may be modeled as a memory function in a simple resistive element. Applying a bias voltage across the anode and cathode creates an electrically conducting resistive bridge. When this bias voltage is removed, the resistive bridge remains intact, so the MIM element remembers the application of the bias voltage. The bridge may be removed by decreasing the bias voltage to zero, which causes the copper atoms in the bridge to disassociate and the nanofilament to decrease in size and

separate from the anode. The applied bias voltage is thus an effective "WRITE" command to the MIM memory element, and the decreased bias is an effective "ERASE" command. Based on this effect, the stabilization of the MIM device I/V characteristic at G_0 or several G_0, rather than at tens of used G_0 in current devices, may allow the near-term implementation of low power digital and analog memristor devices.

4. It is important to note that a reverse bias is not necessarily required to rupture the conducting bridge and ERASE the stored data. This means that only a single polarity voltage is required by the IC, and this simplifies system electronics.

As an example of our measurements of memristor memory cell performance, Figure 37 shows the switching transient behavior of one of our test elements. The top curve is the input 2V voltage pulse with a width of 500ns to write the device from the OFF state to the ON state. The bottom curve is the measured voltage across a resistor in series with the memory device. The risetime difference between the input signal (top curve) and the output signal (bottom curve) is about 80ns, indicating a WRITE speed of about 80ns. Importantly, write speed is proportional to the square of the voltage. Current representative commercial rad hard memory devices operate at 5V, and have a write speed of 140ns[2]. At 5V, our device would have a WRITE speed of about $(80ns)/[(5V)^2/(2V)^2] = 13ns$, or about ten times faster. Bias voltage and device response speed can thus be traded off for improved performance over existing rad hard memory devices.

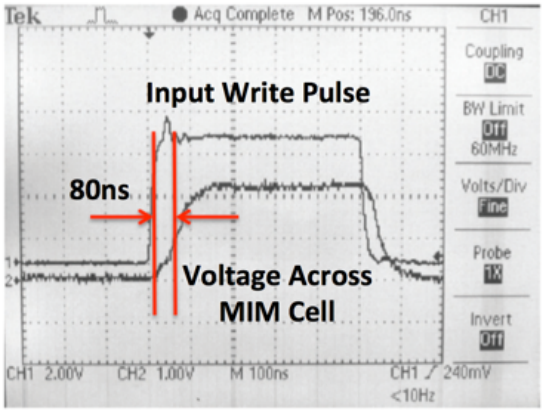

Figure 37: Determination of Switching Speed of NanoSonic MIM Memory Element.

Our understanding of these effects have involved studying the non-linearities in current voltage characteristics at source-drain bias voltages (V_{sd}) where quantized conductance is observed. This requires measuring the differential conductance dI/dV_{sd} at fixed bias V_{sd}, where I is the current from the source to drain in the two-terminal devices. In narrow 1-D electron waveguide constrictions at high bias V_{sd} where the non-linearity appears, one indeed has to distinguish between the conductance I/V_{sd} (reported so-far)

[2] https://aerospace.honeywell.com/en/~/media/.../mram-sales-sheet-july-2015-bro.pdf

and the differential conductance dI/dV_{sd} measured at fixed bias V_{sd}, because conductance and differential conductance are differently sensitive to the relative values of the two relevant energy scales: eV_{sd} and one-dimensional subband energy spacing in the constriction. Such a bias spectroscopy can reveal important information about the origin of fractional quantized conductance and non-linearities.

III. SBIR PROGRAM SUMMARY

The objective of this Department of Energy SBIR program has been to develop technology for the advancement of advanced computing systems. NanoSonic worked with two subcontractors, the Polymicro Division of Molex, a U.S.-based manufacturer of specialized optical fiber and fiber components, and Virginia Tech, a research university involved through the Global Environment for Network Innovations (GENI) program in high-speed computer networking research.

NanoSonic developed a patented molecular-level self-assembly process to manufacture polymer-based optical fibers in a way similar to the modified chemical vapor deposition (MCVD) approach typically used to make glass optical fibers. Although polymer fiber has a higher attenuation per unit length than glass fiber, short connectorized polymer fiber jumpers offer significant cost savings over their glass counterparts, particularly due to the potential use of low-cost plastic fiber connectors. As part of the SBIR commercialization process, NanoSonic exclusively licensed this technology to United Technologies, a large ($100B+ market cap) U.S.-based manufacturing conglomerate near the end of the first year of the Phase II program.

With this base technology developed and licensed, NanoSonic then worked with Molex/Polymicro to address secondary program goals of using related but not conflicting production methods to enhance the performance of other specialty optical fiber products and components, and Virginia Tech continued its evaluation of developed polymer fibers in its network infrastructure system on the university campus.

The results of that work included the following.

- Demonstration of zero failures in NanoSonic fabricated fiber jumpers at Virginia Tech through testing of approximately 10,000 hours.
- Testing of GaIn metal fiber coatings by Polymicro.
- Testing of hydrogen impermeable fiber coatings by Polymicro.
- Testing of high temperature fiber coatings, higher than commercial polyimide, by Polymicro.

Although NanoSonic has not licensed any of the additional technology developed during the second year of the program, several proprietary discussions with major materials companies, sales of developed materials, and discussions of additional licensing are underway as of the conclusion of Phase II.